ABUAD Journal of Engineering Research and Development (AJERD)
ISSN (online): 2645-2685; ISSN (print): 2756-6811

Volume 7, Issue 2, 521-531

Characterization of Rice Husk for Graphene Extraction and Metallization

Harrison Okechukwu ONOVO[1], Ademola Abiona AGBELEYE[1], Theddeus Tochukwu AKANO[2], Olamilekan Razak OLOYEDE[3], Solomon Onaolapo OYEGBAMI[4], Emmanuel Oluwatimilehin AMOO[1],

[1]*Department of Metallurgical and Materials Engineering, Faculty of Engineering, University of Lagos 101017, Nigeria*
honovo@unilag.edu.ng/aagbeleye@unilag.edu.ng/amooemma10@gmail.com

[2]*Department of Mechanical Engineering, University of Botswana Gaborone, Botswana*
akanott@ub.ac.bw

[3]*Department of Mechanical and Mechatronics Engineering, Afe Babalola University, Ado Ekiti, Nigeria*
engrlekanoloyede@yahoo.com

[4]*Department of Metallurgical and Materials Engineering, College of Engineering, Yaba College of Technology, Lagos Nigeria*
niyioyegbami@gmail.com

Corresponding Author: honovo@unilag.edu.ng, +2348035925649
Date Submitted: 29/10/2024
Date Accepted: 09/12/2024
Date Published: 26/12/2024

Abstract: *Rice husk, an underutilized agricultural waste product, serves as a potential precursor for graphene synthesis. This study focuses on synthesizing and characterizing graphene through the chemical exfoliation method, employing advanced analytical techniques to explore its potential applications in metallization. Graphene was produced by chemically activating rice husk ash (RHA) with potassium hydroxide (KOH) at 800 ºC. The extracted graphene underwent analysis using various techniques. X-ray Diffraction (XRD) confirmed the material's crystalline nature and graphitic structure. Fourier-Transform Infrared Spectroscopy (FTIR) identified typical functional groups present in the synthesized graphene. Raman Spectroscopy revealed significant defects and confirmed that the graphene consists of single or few-layer thin sheets. Transmission Electron Microscopy (TEM) showed the presence of thin graphene sheets and nanoparticles with sizes ranging from 1.47 nm to 5.80 nm. Ultraviolet-Visible Spectroscopy (UV-Vis) confirmed electronic structure and optical properties, essential for metallization. X-ray Fluorescence (XRF) confirmed the purity of the graphene, while Brunauer-Emmett-Teller (BET) analysis revealed a high specific surface area, making the material suitable for surface-based applications. Electrical conductivity tests demonstrated good conductivity in the lower to moderate current range. The study underscores the potential of rice husk-derived graphene for metallization, offering a cost-effective and eco-friendly synthesis method for industrial and commercial applications.*

Keywords: *Agricultural Waste, Chemical Exfoliation, Graphene, Metallization, Potassium Hydroxide, Rice Husk*

1. INTRODUCTION

Biomass refers to organic material derived from plants or animals that can be converted into energy or used in industrial processes. As a renewable resource, biomass plays a crucial role in promoting a sustainable and circular economy. Major sources of biomass include agricultural residues like rice husk, corn stalks, and sugarcane bagasse, as well as forestry residues, industrial organic waste, and municipal solid waste. In contrast to fossil fuels, which require millions of years to form and are finite, biomass is continually replenished through natural processes like photosynthesis [1,2]. Given the growing global population and increasing demand for energy, materials, and food, converting biomass into usable products is becoming essential for reducing environmental pressures and fostering sustainable development [3,4].

Agricultural waste is a significant source of biomass, produced in large quantities due to the rapid expansion of farming. This waste includes materials like rice husk, wheat straw, maize stalks, and sugarcane bagasse, much of which is typically burned, left to decompose, or sent to landfill practices that can cause environmental harm [5]. However, agricultural waste also offers opportunities for innovation. Through the use of appropriate technologies, this waste can be transformed into valuable products, contributing to both environmental sustainability and economic growth. Moreover, transforming waste to resources helps to achieve SDGs 3 and 11. This shift from waste to resource aligns with the circular economy principles, which encourage the reuse, recycling, and regeneration of materials in a closed-loop system, minimizing the need for new raw materials and reducing waste [6].

Rice husk, a byproduct of rice milling, is one such waste material that has traditionally had limited uses. Recent research, however, has highlighted its potential as a source of high-quality graphene, a material renowned for its exceptional electrical, mechanical, and thermal properties [7]. The process of synthesizing graphene from rice husk not only addresses waste disposal issues but also supports global sustainability goals, such as those outlined in the United Nations' Sustainable Development Goals (SDGs) 3 and 11. This is particularly relevant in regions like Abakaliki in Nigeria, where rice milling is widespread, and large quantities of rice husk are generated. Converting this waste into graphene could provide both local and global benefits by contributing to sustainable development and reducing environmental impacts [8].

Rice husk, which makes up about 20% of the total weight of harvested rice [9], generates vast amounts of waste approximately 200 kg for every tonne of rice. In places like Abakaliki, this waste has typically been burned for fuel or discarded, leading to environmental damage and contributing to greenhouse gas emissions [2]. However, rice husk is rich in silica, cellulose, and other organic compounds, making it a promising candidate for research aimed at converting agricultural waste into useful materials [10]. Graphene, which is a single layer of carbon atoms, offers remarkable properties such as high electrical conductivity, mechanical strength, and flexibility, making it a promising material for various sectors, particularly electronics and energy storage [11].

Graphene synthesized from rice husk presents a sustainable and cost-effective alternative to traditional materials like gold and copper, which are widely used in microelectronics. With its superior electrical conductivity, graphene is capable of surpassing copper in enabling efficient current flow within electronic circuits. Furthermore, graphene's resistance to corrosion and degradation makes it suitable for long-term applications. The growing demand for smaller, faster, and more energy-efficient devices has spurred interest in using graphene in the microelectronics industry, where its unique properties could revolutionize fields ranging from flexible electronics to integrated circuits [5].

1.1 Graphene and its Properties

Graphene, a two-dimensional carbon-based material, has revolutionized modern research with its exceptional properties. First theorized by Wallace [12] in 1947 while studying graphite's electrical structure, graphene was later successfully isolated by Geim and Novoselov in 2004, earning them the Nobel Prize in Physics [12]. It consists of sp^2-bonded carbon atoms arranged in a hexagonal honeycomb lattice, classifying it as a two-dimensional material [13]. Graphene's unique band structure, where conduction and valence bands meet at the Dirac point, allows for extraordinary electrical conductivity, charge carrier mobility, and optical transparency, making it suitable for numerous applications in electronics, energy storage, and more [14].

In addition to its electrical properties, graphene exhibits outstanding thermal conductivity, surpassing traditional materials like graphite. The thermal conductivity of single-layer suspended graphene ranges from 4,800 to 5,300 W/m^oK at room temperature, compared to 2,000 W/m^oK for graphite [15]. The size and number of graphene layers influence this property, with smaller, fewer layers showing higher thermal conductivity due to reduced phonon scattering [16].

Graphene's optical properties are equally impressive, as it absorbs approximately 2.3% of visible light per layer, allowing multilayer samples to remain highly transparent [17]. Its ability to absorb light across a wide spectral range from visible to infrared makes it useful in optoelectronic applications. Additionally, graphene's strength is unmatched; it has a tensile strength of 130 GPa, making it 200 times stronger than steel [18].

Due to its two-dimensional structure, every atom in graphene is exposed to chemical reactions, enhancing its reactivity compared to other carbon-based materials. The π electrons in graphene further strengthen its carbon-carbon bonds, contributing to its high mechanical and chemical stability [19].

Graphene's exceptional properties, such as its strength, conductivity, and transparency, make it a promising material for future technological innovations. With potential applications spanning across industries like microelectronics, energy storage, and advanced materials, it is poised to revolutionize these sectors. This study, therefore, seeks to investigate the green synthesis of graphene from rice husks and explore its potential applications in the rapidly evolving microelectronics industry.

2. MATERIALS AND METHODS

2.1 Materials

During the study, the materials used were; rice husk sourced from Abakaliki in Ebonyi State of Nigeria, Potassium Hydroxide, Glass wool, distilled water, and deionised water bought from a chemical store market in Idumota, Lagos State, Nigeria. Fire clay was obtained from Abeokuta, Ogun State of Nigeria while the clay pot was purchased in Bariga market, Lagos, Nigeria.

2.2 Methods

2.2.1 Synthesis of graphene

The rice husk waste acquired was pulverized, properly washed under a tap running water, and later rinsed in deionized water to eliminate dust, silica, and other impurities. It was then oven-dried at 120 °C for 2 hours to remove all moisture and other impurities containing silica. The dried husk was then compacted, covered in a ceramic crucible, and carbonized in a furnace at 400 °C for 2 hours to obtain RHA as contained in Figure 1 (a- d). This technique of graphene synthesis from rice husk is in line with the proposed process by Muramatsu *et al* [5] but with some modifications. The equation for the reaction is given in Equation 1 and 2.

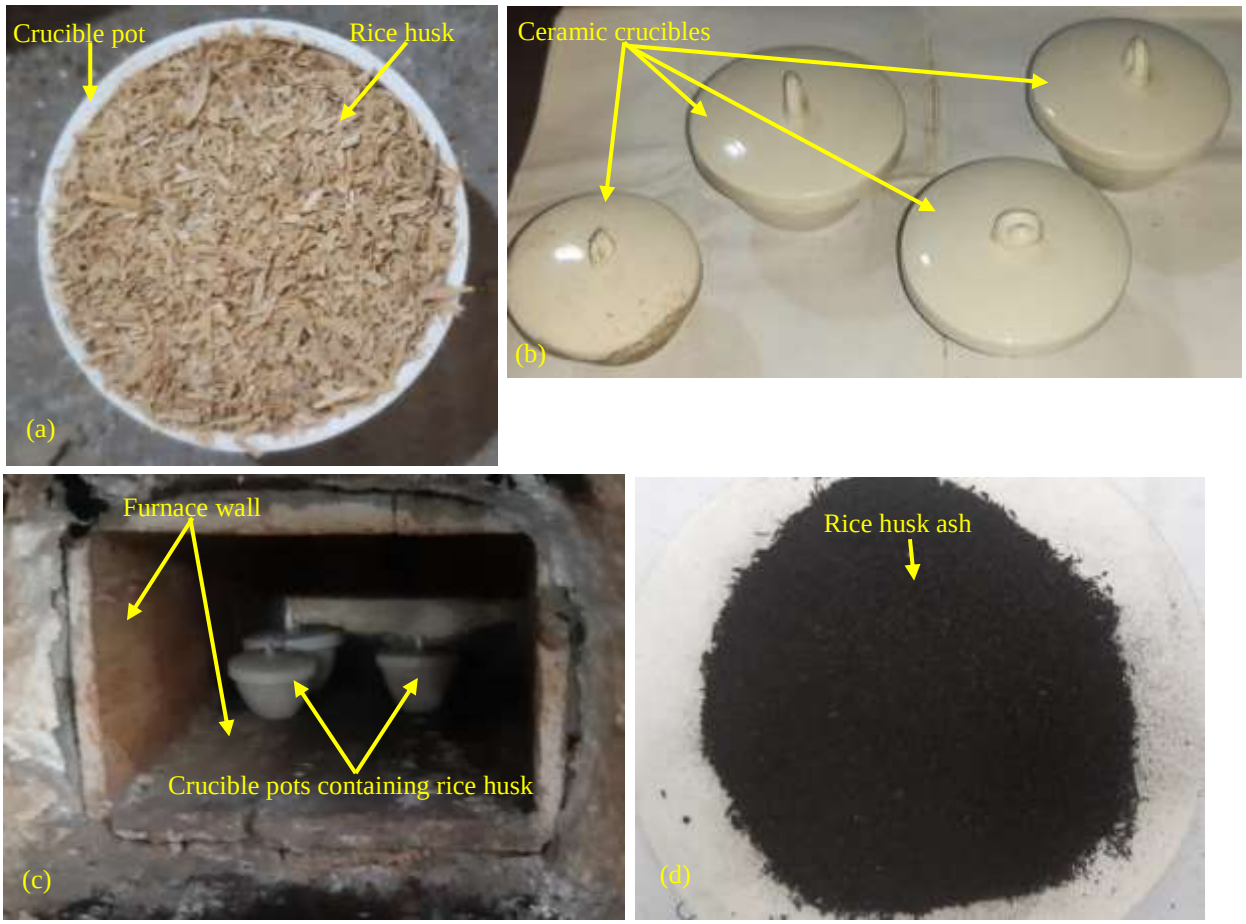

Figure 1: Ashing process of rice husk in the furnace: (a) oven-dried rice husk in a ceramic crucible pot, (b) covered ceramic crucible pots with dried rice husk, (c) ceramic crucible pots in the furnace, and (d) RHA

$$\text{Rice Husk} + \text{Heat} \rightarrow \text{RHA}\ (\text{C} + \text{SiO}_2) \quad (1)$$

$$\text{C}_6H_{10}O_5 + Heat \rightarrow 6C + 5H_2O + volatile\ gases \quad (2)$$

The RHA was chemically activated with KOH powder of a 1:5 impregnation ratio, as shown in Equations 3 and 4 which present the reaction procedures

$$6\text{KOH} + \text{Si}O_2 \longrightarrow K_2SiO_3 + 3H_2O \quad (3)$$

$$6\text{KOH} + 2\text{C} \longrightarrow 2K + 3H2 + 2K_2CO_3 \quad (4)$$

The mixture was then placed into a ceramic crucible and sealed with a lid. The ceramic crucible was placed in the middle of a clay pot, with the sides well sealed with very fine fire clay. Thereafter, the sides of the clay pot were also sealed in the same manner, as demonstrated in Figures 2 (a-d). The essence of the two-stage sealing of the pots (crucible and clay) is to create an adiabatic system, where even the atomized air or gas penetration or escape is drastically prevented during the 2 hours furnace heating reaction at 800 °C (Figure 3) and cooling regime. Equation 5 shows the reaction for porous carbon formation. The overall reaction process is depicted in Equation 6, and Figures 3(a-h) illustrate the entire procedure

$$K_2CO_3 + 2C \longrightarrow 2K + 3CO\ (Formation\ of\ porous\ carbon) \quad (5)$$

$$C_6H_{10}O_5 + SiO_2 + KOH \longrightarrow C(\text{Graphene} - \text{like carbon}) + K_2SiO_3 + CO + K_2CO_3 + H \quad (6)$$

Once the reaction was complete, the pot was cooled in the furnace. The sample obtained was scooped into a beaker with 50 ml added and it was stirred for 5 hours with a magnetic stirrer. The solution was filtered and repeatedly rinsed with

distilled water to eliminate any remnant of KOH until it reached a pH of 7. The graphene obtained was then dried in an oven at 80 °C for 8 hours to remove excess moisture.

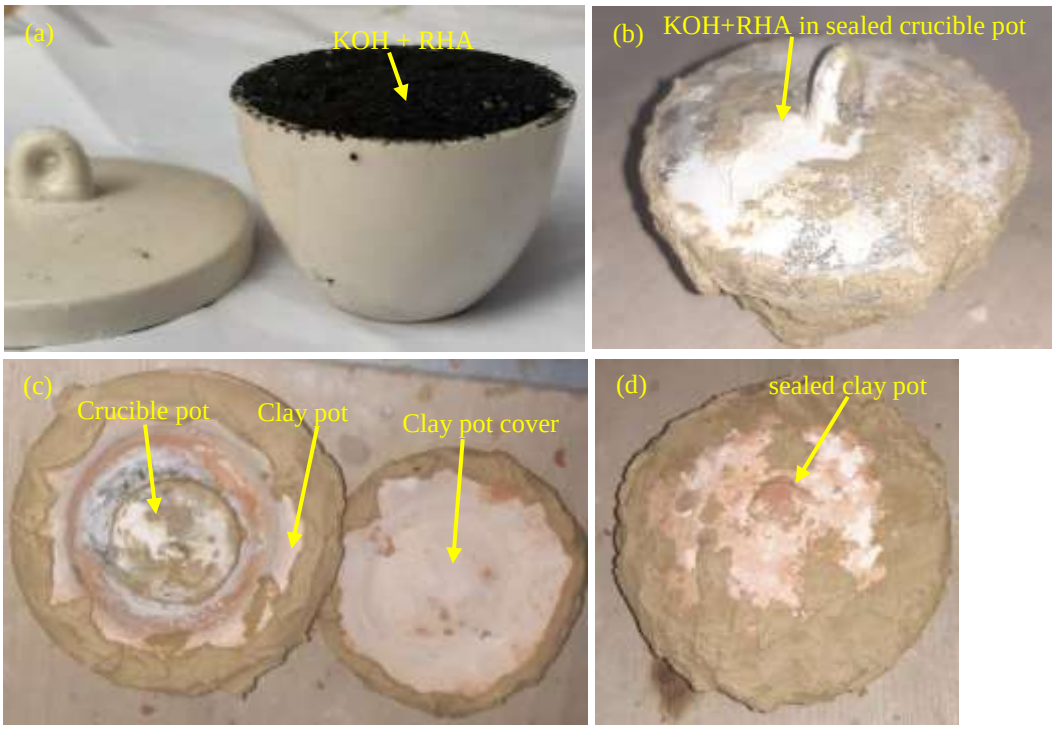

Figure 2: RHA activation with KOH of 1:5 impregnation ratio: (a) mixture of KOH and RHS in crucible pot, (b) mixture of KOH and RHA, (c) crucible pot inside clay pot, and (d) sealed clay pot containing crucible pot with mixture of KOH and RHA.

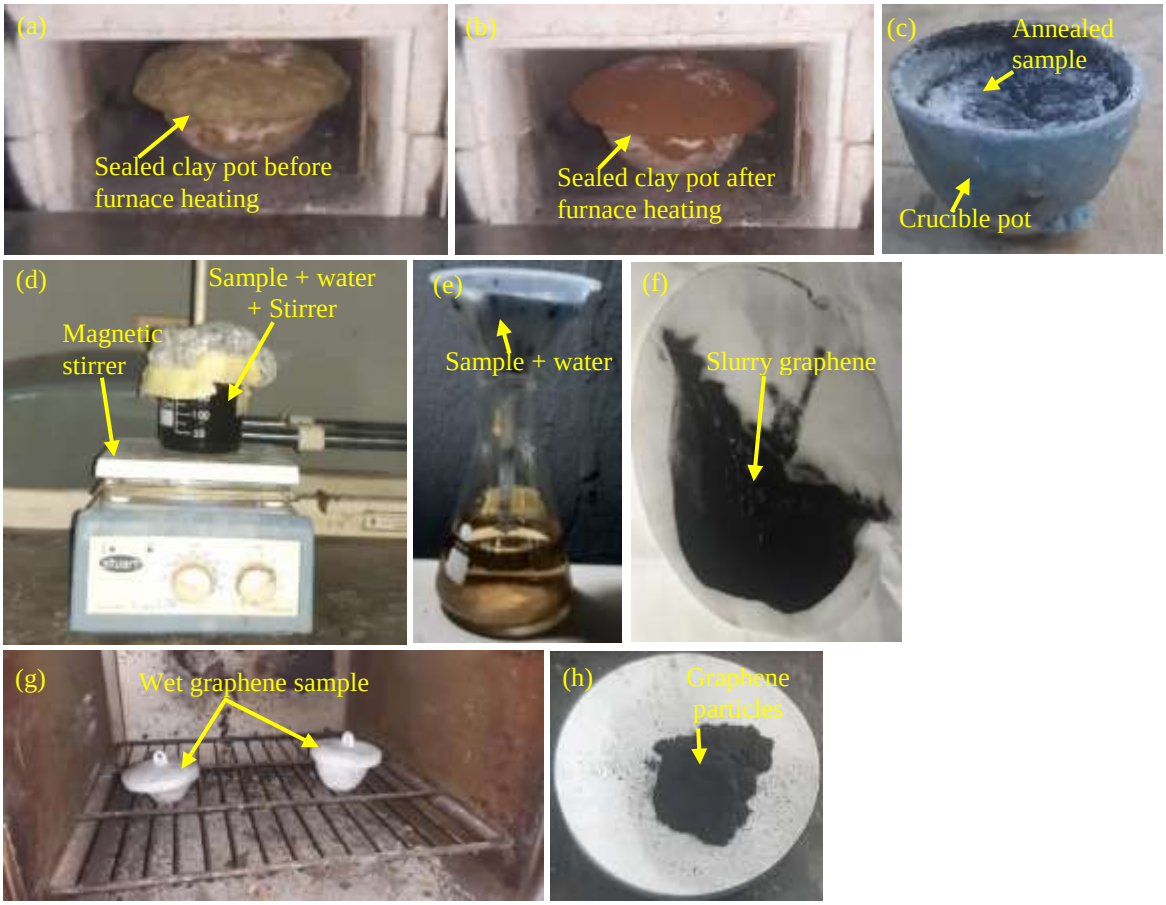

Figure 3: Annealing procedures for graphene sample: (a) clay pot inside the furnace before heat treatment, (b) after heat treatment, and (c) crucible pot with annealed graphene, (d) wet graphene on magnetic stirrer, (e) graphene filtration, (f) slurry graphene, (g) crucible pot with wet graphene for oven drying, and dried graphene

Graphene obtained from the synthesis of rice husk and chemically activated with potassium hydroxide is blackish in color. The process entails the pulverization of rice husk obtained from the mill, followed by washing in deionized water. The rice husk was dried in a furnace and heated for 2 hours at 400 °C in a furnace. The RHA was obtained after the carbonization process, followed by chemical activation with KOH with an impregnation ratio of 1:5 of KOH powder which is then heated 800 °C for 2 hours. After that, the sample obtained was stirred in a magnetic stirrer for 5 hours, and washing and neutralization of graphene took place simultaneously. Afterward, the graphene is filtered and dried in an oven at 80 °C for 8 hours to obtain dry graphene. The graphene obtained is black. After that, the sample is metallized on a glass substrate. The sample obtained is characterized by Raman spectroscopy, X-ray diffraction, Transmission electron microscopy, Fourier transform Infrared spectroscopy (FTIR), X-ray Fluorescence (XRF), and Brunauer-Emmett-Teller (BET) analysis. At the same time, a conductivity test was conducted on the metallized material.

2.2.2 Metallization of graphene on glass

The insulator material (glass) was cleaned and dried to ensure a smooth and clean surface. Then, the epoxy was mixed with hardener in preparation for the application of the graphene powder. Thereafter, graphene powder was applied onto the glass surface using epoxy as the adhesive as shown in Figure 4. The material was heated to 230 °C for adhesion and also to remove any remaining solvent and improve the graphene's conductivity.

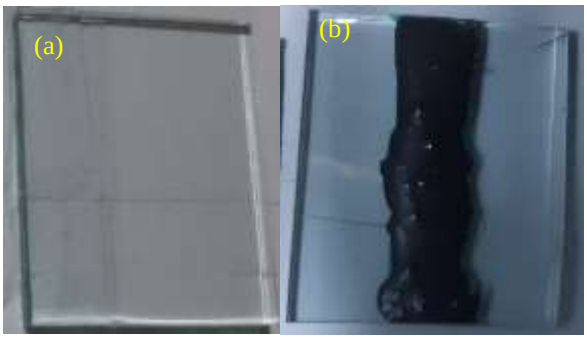

Figure 4: Steps for glass surface metallization with graphene: (a) prepared glass surface, and (b) glass surface coated with graphene-rich epoxy mixture.

2.2.3 Characterisation process

Graphene synthesized from rice husk was characterized using various analytical techniques. Raman spectroscopy was performed with the OPTOSKY Raman microscopy ATR8500, while UV-visible spectroscopy (UV-Vis) was carried out using the LAMBDA 1050+ UV/Vis/NIR Spectrophotometer (L6020055). X-ray diffraction (XRD) analysis was conducted using the Empyrean X-ray Diffraction Alpha-1 system. Fourier Transform Infrared Spectroscopy (FTIR) was performed with the Shimadzu IRTracer-100. The microstructure and average particle size of the graphene were analyzed using the JEM-1400Flash Transmission Electron Microscope (TEM). Elemental composition was examined with X-ray Fluorescence (XRF) using the NEX QC+ QuantEZ Advanced EDXRF Analyzer. Additionally, the Brunauer-Emmett-Teller (BET) analysis was used to determine particulate sizes. The conductivity of the metallized graphene material was also evaluated.

3. RESULT AND DISCUSSION

3.1 X-Ray Fluorescence (XRF)

The XRF (X-ray Fluorescence) analysis of the graphene sample reveals the presence of several compounds, with SiO_2 (34.89 wt%) and K_2O (26.99 wt%) being the most abundant. Other significant compounds include CaO (8.62 wt%), Al_2O_3 (12.32 wt%), and MgO (3.87 wt%). The presence of these oxides, particularly SiO_2 and K_2O, indicates that the graphene contains impurities from the rice husk (Figure 5). Smaller quantities of other elements, such as Fe_2O_3, TiO_2, and ZnO, further suggest that the sample is not purely graphene but contains various mineral and metal oxides. This composition is typical for graphene synthesized from rice husk biomass.

3.2 Transmission Electron Microscopy (TEM)

The TEM (Transmission Electron Microscopy) images show various critical properties of graphene made from rice husk. The supplied measurements show that the graphene particles range in size from 1.47 nm to 5.80 nm. This size difference shows that the manufacturing procedure resulted in graphene sheets with different lateral dimensions. The particles appear to be spherical or nearly spherical, which indicates that the graphene sheets are crumpled or folded. This is typical in reduced graphene oxide (rGO) and other chemically produced graphene materials, where the sheets fold to create compact formations [16]. Some sections have somewhat extended or irregular shapes, which could indicate the presence of multi-layered graphene. The smallest particle sizes (for instance, 1.47 nm and 1.89 nm) are consistent with single- or few-layer graphene, indicating that the synthesis procedure created thin graphene sheets. The larger particles such as 5.80 nm could represent multi-layer graphene or thicker stacks of graphene sheets.

Particles of different sizes and shapes indicate the presence of flaws or functional groups on the graphene surface. These flaws are most typically created during the synthesis process's oxidation or reduction stages [17]. TEM images shown in Figure 6 (a and b), indicate that graphene produced from rice husk contains both single-layer and few-layer graphene particles [18]. Particle size and shape variations are consistent with chemically produced graphene, which frequently has variable layer counts and a certain degree of defects [8].

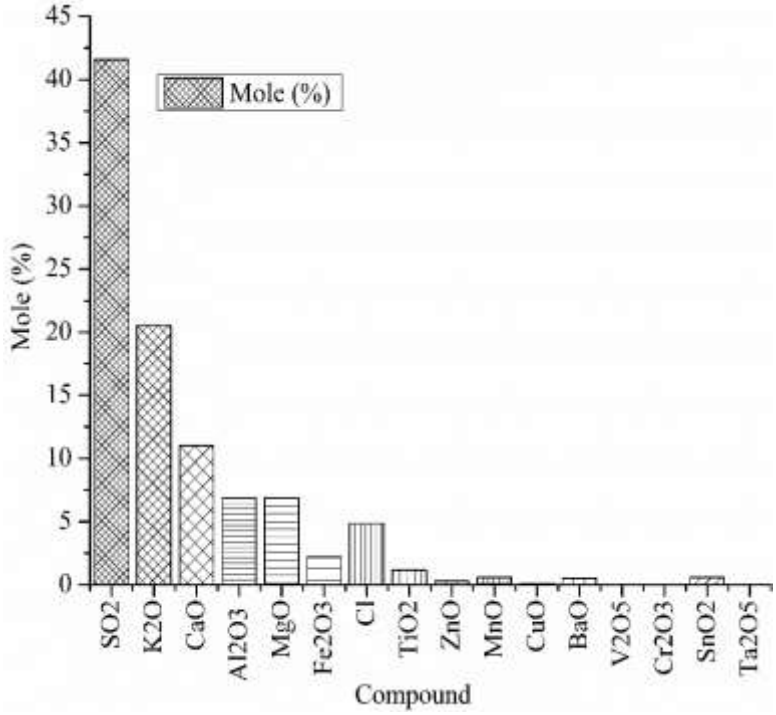

Figure 5: Compounds in the sample (XRF)

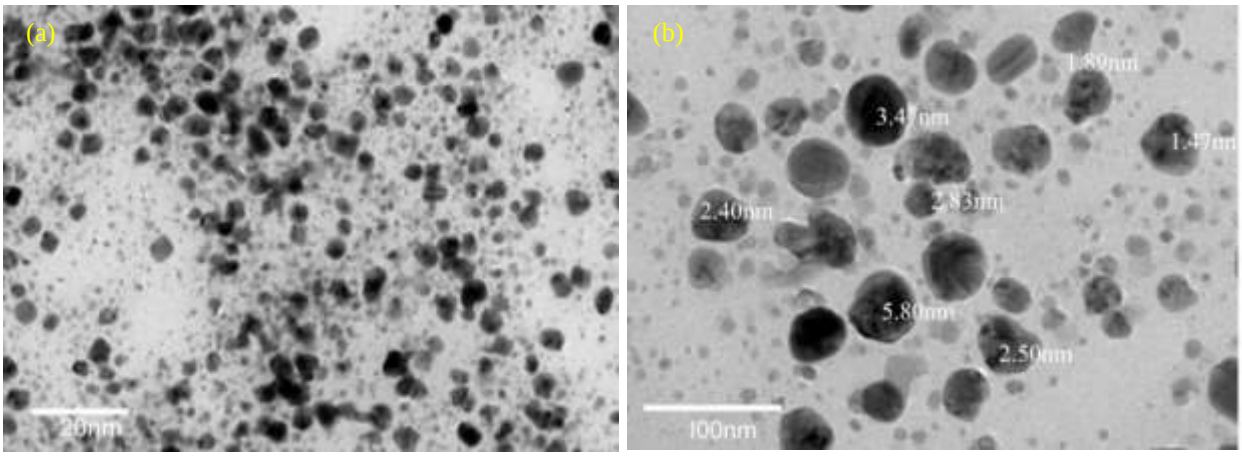

Figure 6: TEM Images at (a) 20nm and (b) 100nm

3.3 Brunauer-Emmett-Teller (BET) Analysis

Using gas adsorption measurements, BET analysis is often used to evaluate the specific surface area of solid materials. The surface area of Single-Point BET is 140.4 m²/g, Multi-Point BET is 247.9 m²/g, and Langmuir Surface Area is 321.4 m²/g, indicating that graphene has a large surface area. A large surface area benefits applications like catalysis, metallization, supercapacitors, or adsorption, as it provides more active sites. The Micropore Area (DR Method) is 254.7 m²/g which is close to the MultiPoint BET surface area, specifying that a major portion of the surface area originates from micropores, which are pores with diameters less than 2 nm. The DFT Cumulative Surface Area is 267.0 m²/g, confirming graphene's high surface area. The huge surface area, particularly the micropore area, indicates that graphene is appropriate for electronic applications.

For the pore volume analysis, the Cumulative Adsorption Pore Volume (BJH and DH Methods) is approximately between 0.127-0.130 cc/g. These results indicate that the graphene has a good amount of meso-porosity. For the DR Method, the micropore volume is 0.0905 cc/g, indicating the presence of micropores in the graphene structure, which adds to the graphene's high surface area. The Cumulative Pore Volume for the DFT Method is 0.0668 cc/g, which is an estimate

of the total pore volume of the material. The coexistence of micropores and mesopores with such high cumulative pore volume infers that graphene obtained from rice husk has a well-developed porous structure. The Pore Diameters for the BJH/DH method are 2.153 nm, the DR method is 6.366 nm, the HK method is 1.847 nm, and the DFT method is 2.647 nm. The graphene obtained exhibits a range of pore sizes, with mesopores around 2 nm being the most prominent, as specified by the BJH, DH, and DFT methods.

3.4 X-Ray Diffraction

The XRD pattern of graphene produced by activating RHA with KOH at 800˚C is displayed in Figure 7. In this analysis, copper (Cu) was used as the anode material. The K-Alpha1 wavelength is 1.54060 Å, while the K-Alpha2 wavelength is 1.54443 Å. The K-Beta wavelength is 1.39225 Å, and the K-A2/K-A1 ratio is 0.50000. The XRD spectra in Figure 7 show a significant peak around 2θ = 26 degrees assigned to the reflection plane of (002) for graphene. The peak represents the presence of a highly organized, layered structure of carbon atoms, which is characteristic of graphene and graphite. The absence of other major peaks in the XRD pattern indicates that the sample has few crystalline impurities, supporting the presence of graphene above other crystalline components. The overall shape and strength of the peaks indicate that the sample contains a large quantity of graphene or graphite-like material. The primary peak confirms the organized carbon structure typically seen in graphene.

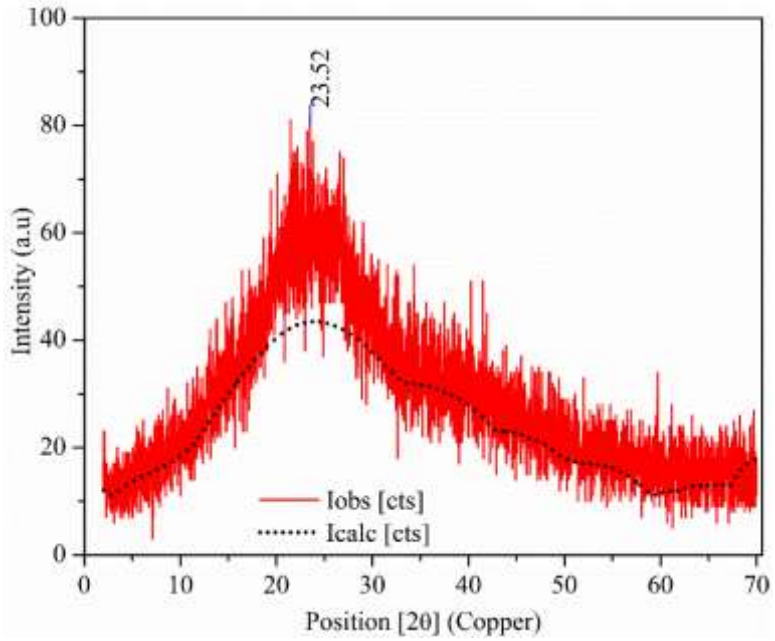

Figure 7: XRD spectra of graphene from rice husk

3.5 Fourier-Transform Infrared Spectroscopy (FTIR)

The FTIR spectra of graphene indicate the presence of some characteristic peaks due to specific functional groups, thereby confirming the synthesis of graphene as shown in Figure 8. When analyzing graphene's FTIR spectra, certain characteristic peaks can be observed. These peaks correspond to specific functional groups present in the material, and they help to identify the chemical structure and confirm the successful synthesis of graphene.

Analysis of Peaks:

a. 905 cm^{-1} (C=C out-of-plane bending vibration): The peak is related to the out-of-plane bending vibrations of C=C bonds found in alkenes, indicating aromatic structures within the graphene framework.
b. 1752 cm^{-1} (C=O stretching vibration): The peak around 1762 cm^{-1} is commonly attributed to C=O stretching vibrations, often found in aldehydes, ketones, and possibly carboxylic acid groups. This might indicate partial oxidation of graphene to give carbonyl groups.
c. 2329 cm^{-1} (O-H stretching vibration with weak hydrogen bonding): This band may indicate the existence of hydroxyl groups (O-H), which could be attributed to residual moisture or possibly alcohols or phenolic groups within the graphene oxide structure.
d. 2665 cm^{-1} (C-H stretching vibration in carboxylic acid dimers): This band at 2663 can be assigned to C-H stretching in carboxylic acid dimers, indicating some level of oxidation in the graphene, leading to carboxyl functionalization.
e. 3680 cm^{-1} and 3971 cm^{-1} (O-H stretching vibrations): These peaks are generally indicative of O-H stretching, which can be linked to various functional groups like alcohols, phenols, and water. These could be due to hydroxyl groups on the graphene oxide surface or adsorbed water in the context of graphene.

Uda *et al*. [19], synthesized graphene from rice husk and identified similar functional groups, particularly noting the presence of C=O and O-H groups, which indicate oxidation during the production process. The existence of these groups

agrees with the formation of graphene from rice husk. Manpetch, Singhapong, and Jaroenworaluck [20] also reported on FTIR spectra of graphene oxide synthesized from rice husk, identifying peaks for C=O and O-H groups, aligning with the typical signatures of graphene oxide and its derivatives. These references support the interpretation of the FTIR peaks, indicating that the graphene contains typical functional groups associated with graphene and graphene-class materials, including carbonyl and hydroxyl groups. This is consistent with other studies on rice husk-derived graphene.

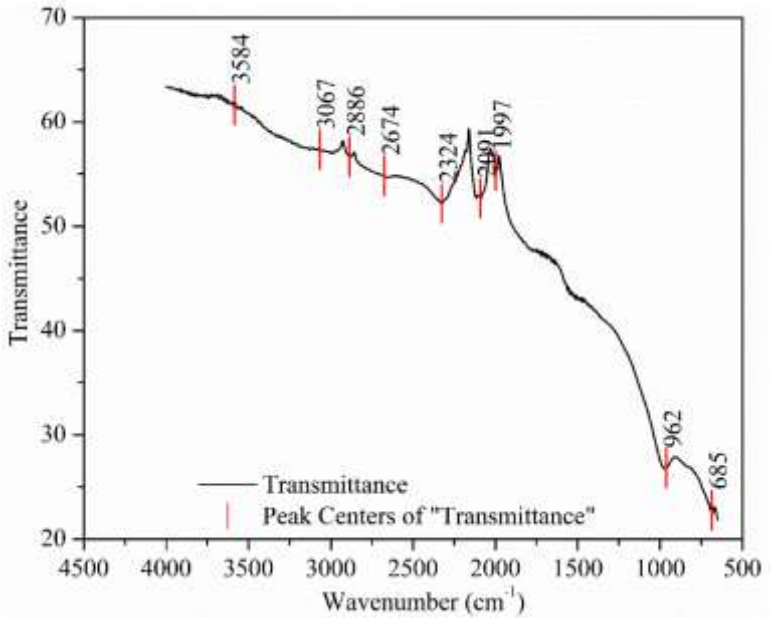

Figure 8: FTIR analysis of graphene from rice husk.

3.6 Ultraviolet-Visible Spectroscopy (UV-ViS)

The UV-Vis absorption spectrum displays in Figure 9 the absorbance of graphene produced from rice husk as a function of wavelength. At the beginning of the spectrum, between 200 and 300 nm, the sample has an absorbance value close to 10 which indicates significant light absorption in the ultraviolet (UV) region. This high absorbance can be attributed to π-π* electrical transitions of the sp^2-bonded carbon atoms in graphene's aromatic structure. The elevated, uniform absorption signifies a substantial density of electronic states within this energy range, aligning with graphene's distinctive band structure.

Beyond 300 nm, absorption drops sharply to less than one. This sharp drop is related to the transition from π→π* electronic excitations to lower energy transitions, signifying that the π-π* transitions decrease as the wavelength increases. This dip shows that the graphene sample has a lower absorbance in the visible region.

From 300 nm to 800 nm, the absorbance stabilizes at a significantly lower level, staying below one. This consistent, low absorbance in the visible to near-infrared region specifies that the graphene sample does not absorb much light in this range. This behavior is characteristic of graphene, which is normally transparent to visible light yet exhibits substantial UV absorption due to the previously stated electrical transitions.

The spectrum indicates that the graphene obtained from rice husk primarily absorbs in the UV region, which is compatible with the presence of conjugated π-systems typical in graphene structures. The sharp drop in absorbance after the UV region indicates that the material does not have significant electronic transitions that absorb in the visible region, confirming the presence of pure or minimally functionalized graphene.

3.7 RAMAN Spectroscopy

The Raman spectrum of graphene produced from rice husk exhibits a sharp D-band at 1292 cm^{-1} (Figure 10), which indicates the presence of structural defects, including edges and functional groups, common in biomass-derived graphene [21,22]. This level of disorder is expected in graphene produced from rice husk due to its high defect density. The 2D-band observed at 2872 cm^{-1} suggests the presence of single-layer graphene [23,24], indicating successful exfoliation. However, the G-band at 1580 cm^{-1}, usually associated with sp^2-bonded carbon atoms, is either absent or faint. This could be due to high levels of disorder, with the D-band dominating the spectrum, or instrument-related issues like laser power or resolution during measurement [24,25]. Such characteristics are typical of graphene synthesized from biomass sources, where the material exhibits more imperfections than physically exfoliated graphene [26-28].

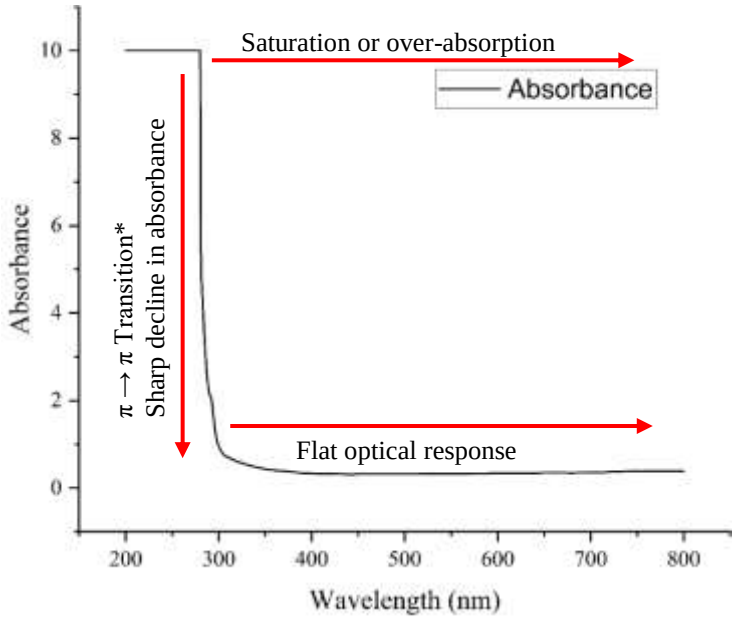

Figure 9: UV-Vis of graphene obtained from rice husk.

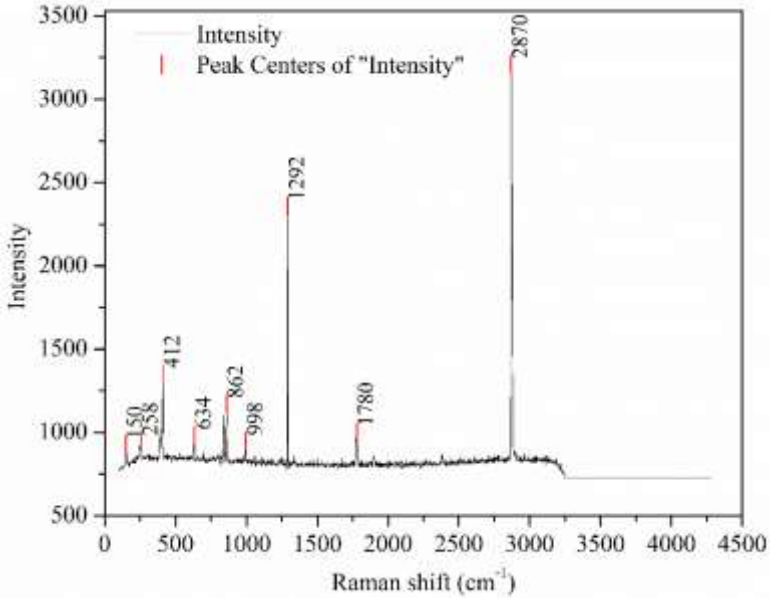

Figure 10: Raman spectroscopy of graphene from rice husk.

3.8 Electrical Conductivity Analysis

From Figure 11, it is evident that at very low current (around 0-100 A), there is a rapid decrease in resistivity from around 3.1 μΩ to below 1.0 μΩ. Simultaneously, the conductivity increases sharply, indicating an increase in the material's ability to conduct electricity as current is applied. Between 100A and 200A, both resistivity decreases more gradually, and conductivity continues to rise. The material's conductivity at this range approaches 4.8 S/m. The decreasing resistivity shows that the graphene's electron mobility is improving under the influence of increased current. From 200 A to 500 A, resistivity continues to decrease slowly, reaching a final value near 1.0 μΩ at 500 A. Conductivity increases further and reaches around 5.0 S/m by 500 A, implying that the material's conductive properties improve significantly under higher current application.

The graph shows the expected inverse relationship between resistivity and conductivity. The significant drop in resistivity with increasing current suggests that metallized graphene behaves similarly to conductive materials, with improved conductivity under higher applied currents. The metallization enhances the graphene's electrical properties by increasing the number of free charge carriers, allowing for greater conductivity as current is applied.

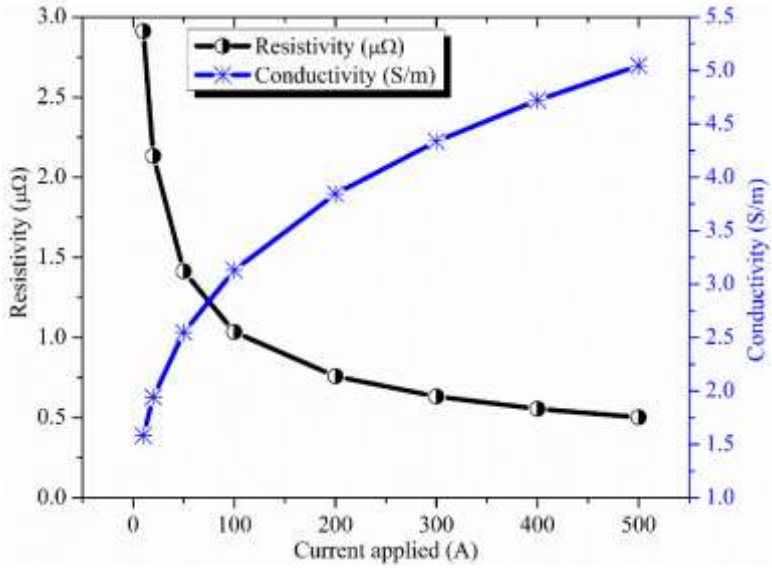

Figure 11: Effect of applied current on conductivity and resistivity.

4. CONCLUSION

The study successfully synthesized graphene from rice husk, characterized by a range of advanced analytical techniques. XRF analysis confirmed the presence of silica (SiO_2, 34.89 wt%) and potassium oxide (K_2O, 26.99 wt%) as dominant compounds, alongside smaller quantities of other metal oxides, indicating residual impurities from the rice husk precursor. TEM analysis revealed graphene particle sizes ranging from 1.47 nm to 5.80 nm, with evidence of single- and few-layer graphene as well as some multilayered structures. The crumpled morphology observed aligns with chemically produced graphene. BET analysis showed a high surface area (up to 321.4 m^2/g) with significant microporosity, suggesting suitability for applications in catalysis, adsorption, and energy storage. Pore analysis indicated mesopores as the predominant feature, with the coexistence of micropores further enhancing surface properties. XRD confirmed the presence of a highly organized carbon structure, typical of graphene, with minimal crystalline impurities. FTIR and Raman spectroscopy identified functional groups such as hydroxyl and carbonyl, along with structural defects, common in biomass-derived graphene. UV-Vis analysis demonstrated strong absorption in the UV region, consistent with graphene's electronic transitions. Electrical testing showed an inverse relationship between resistivity and conductivity, with conductivity reaching 5.0 S/m at higher current levels, indicating enhanced electrical properties due to metallization. Overall, the synthesized graphene exhibits promising structural, chemical, and electrical characteristics, making it a viable candidate for applications in metallization, electronics, and energy storage systems.

ACKNOWLEDGMENT

The authors would like to express our sincere gratitude to Dr. Henry E. Mgbemere, Acting Head of the Department of Metallurgical and Materials Engineering, University of Lagos, for providing us with the laboratory facilities necessary to conduct this research. The availability of these resources was instrumental in the successful completion of this study.

REFERENCES

[1] Abhilash, S.V., & Meshram, P. (2021). An overview on chemical processes for synthesis of graphene from waste carbon resources. *Carbon Letters*, *32*(3), 653–669. https://doi.org/10.1007/s42823-021-00313-7.

[2] Lee, S., Lee, S.J., Jung, H.S., Kim, A., Ahmed, A.T.A., Inamdar, A.I. & Kim, D.Y. (2017). Ultrathin graphene nanosheets derived from rice husks for sustainable supercapacitor electrodes. *New Journal of Chemistry (1987)*, *41*(22), 13792–13797. https://doi.org/10.1039/c7nj03136j

[3] Taiwo, A.E., & Musonge, P. (2024). Valorization of Corn Steep Liquor for Improved Value-added Products: A Review, *Recent Innovations in Chemical Engineering*, 17(1), 26 – 43. DOI: 10.2174/0124055204282376231219095404

[4] Taiwo, A.E., Madzimbamuto, T.F. & Ojumu, T.V. (2020). *Development of an Integrated Process for the Production and Recovery of Some Selected Bioproducts from Lignocellulosic Materials*. In: Daramola, M., Ayeni, A. (eds) Valorization of Biomass to Value-Added Commodities. *Green Energy and Technology. Springer, Cham*. https://doi.org/10.1007/978-3-030-38032-8_21

[5] Marinho, B., Ghislandi, M., Tkalya, E., Koning, C. & De With, G. (2012). Electrical conductivity of compacts of graphene, multi-wall carbon nanotubes, carbon black, and graphite powder. *Powder Technology, 221, 351–358.* https://doi.org/10.1016/j.powtec.2012.01.024

[6] Ruiz-Hitzky, E., Aranda, P., Darder, M. & Ogawa, M. (2011). Hybrid and biohybrid silicate based materials: molecular vs. block-assembling bottom–up processes. *Chem. Soc. Rev.*, *40*, 801-828. https://doi.org/10.1039/C0CS00052C.
[7] Muramatsu, H., Kim, Y.A., Yang, K.S., Cruz-Silva, R., Toda, I., Yamada, T. & Saitoh, H. (2014). Rice Husk-Derived Graphene with Nano-Sized Domains and Clean Edges. *Small (Weinheim. Print)*, *10*(14), 2766–2770. https://doi.org/10.1002/smll.201400017.
[8] Zhu, C., Guo, S., Fang, Y. & Dong, S. (2010). Reducing sugar: new functional molecules for the green synthesis of graphene nanosheets. *ACS Nano*, *4*(4), 2429–2437. https://doi.org/10.1021/nn1002387.
[9] Singh, B. (2018). Rice husk ash, Editor(s): Rafat Siddique, Paulo Cachim, In Woodhead Publishing Series in Civil and Structural Engineering, Waste and Supplementary Cementitious Materials in Concrete, *Woodhead Publishing*, 417-460. https://doi.org/10.1016/B978-0-08-102156-9.00013-4.
[10] Naveen, R., Kim, H. & Shahrir, F. (2021). Graphene for next-gen microelectronics. *Advanced Functional Materials*. https://doi.org/10.1002/adfm.202101232.
[11] Wallace, P.R. (1947). The Band Theory of Graphite. *Physical Review*, *71*(9), 622–634. https://doi.org/10.1103/physrev.71.622.
[12] Meyer, J.C., Geim, A.K., Katsnelson, M.I., Novoselov, K.S., Booth, T.J. & Roth, S. (2007). The structure of suspended graphene sheets. *Nature*, *446*(7131), 60–63. https://doi.org/10.1038/nature05545.
[13] Adetayo, A. & Runsewe, D. (2019). Synthesis and Fabrication of graphene and graphene Oxide: a review. *Open Journal of Composite Materials*, *09*(02), 207–229. https://doi.org/10.4236/ojcm.2019.92012.
[14] Geĭm, A.K. (2009). Graphene: Status and Prospects. *Science*, *324*(5934), 1530–1534. https://doi.org/10.1126/science.1158877.
[15] Urade, A. R., Lahiri, I. & Suresh, K. (2022a). Graphene Properties, Synthesis and Applications: A review. *JOM*, *75*(3), 614–630. https://doi.org/10.1007/s11837-022-05505-8.
[16] Seol, J.H., Jo, I., Moore, A.L., Lindsay, L., Aitken, Z.H., Pettes, M.T., & Shi, L. (2010). Two-Dimensional phonon transport in supported graphene. *Science*, *328*(5975), 213–216. https://doi.org/10.1126/science.1184014.
[17] Nair, R.R., Blake, P., Григоренко, A.H., Новоселов, K.C., Booth, T., Stauber, T. & Geĭm, A. K. (2008a). Fine structure constant defines visual transparency of graphene. *Science*, *320*(5881), 1308. https://doi.org/10.1126/science.1156965.
[18] Lee, C., Wei, X., Kysar, J.W. & Hone, J. (2008). Measurement of the elastic properties and intrinsic strength of monolayer graphene. *Science*, *321*(5887), 385–388. https://doi.org/10.1126/science.1157996.
[19] Kaur, R. & Tripathi, S. (2018). Properties and applications of graphene. *Materials Today: Proceedings*. https://doi.org/10.1016/j.matpr.2018.10.215.
[20] Xu, Y., Sheng, K., Li, C. & Shi, G. (2010). Self-Assembled graphene hydrogel via a One-Step hydrothermal process. *ACS Nano*, *4*(7), 4324–4330. https://doi.org/10.1021/nn101187z.
[21] Ferrari, A.C. & Robertson, J. (2000). Interpretation of Raman spectra of disordered and amorphous carbon. *Physical Review. B, Condensed Matter*, *61*(20), 14095–14107. https://doi.org/10.1103/physrevb.61.14095.
[22] Wick, P., Louw-Gaume, A.E., Kucki, M., Krug, H.F., Kostarelos, K., Fadeel, B. & Bianco, A. (2014). Classification Framework for Graphene-Based Materials. *Angewandte Chemie International Edition*, *53*(30), 7714–7718. https://doi.org/10.1002/anie.201403335.
[23] Uda, M. N. A., Gopinath, S. C. B., Hashim, U., Halim, N. H., Parmin, N. A., Uda, M. N. A. & Anbu, P. (2021). Production and characterization of graphene from carbonaceous rice straw by cost-effect extraction. *3 Biotech*, *11*(5). https://doi.org/10.1007/s13205-021-02740-9.
[24] Manpetch, P., Singhapong, W. & Jaroenworaluck, A. (2022). Synthesis and characterization of a novel composite of rice husk-derived graphene oxide with titania microspheres (GO-RH/TiO2) for effective treatment of cationic dye methylene blue in aqueous solutions. *Environmental Science and Pollution Research*, 29(42), 63917–63935. https://doi.org/10.1007/s11356-022-20176-3.
[25] Ferrari, A. C. & Basko, D. M. (2013). Raman spectroscopy as a versatile tool for studying the properties of graphene. *Nature Nanotechnology*, *8*(4), 235–246. https://doi.org/10.1038/nnano.2013.46.
[26] Graf, D., Molitor, F., Ensslin, K., Stampfer, C., Jungen, A., Hierold, C. & Wirtz, L. (2007). Spatially resolved Raman spectroscopy of single- and Few-Layer graphene. *Nano Letters*, 7(2), 238–242. https://doi.org/10.1021/nl061702a.
[27] Malard, L., Pimenta, M., Dresselhaus, G. & Dresselhaus. (2009). Raman spectroscopy in graphene. *Physics Reports*, *473*(5–6), 51–87. https://doi.org/10.1016/j.physrep.2009.02.003.
[28] Gao, W. (2015). The chemistry of graphene oxide. In *Springer eBooks* (61–95). https://doi.org/10.1007/978-3-319-15500-5_3